Transition from Ventricular Tachycardia to Ventricular Fibrillation as Function of Tissue Characteristics in a Computer Model

Flavio H. Fenton[1], Alain Karma[2], Harold M. Hastings[3], and Steven J. Evans[4]

A simplified quantitative ionic model of cardiac action potential, which reproduces accurate restitution curves, is used in conjunction with global tissue characteristics such as rotational cell anisotropy and periodic boundaries to study the transition from ventricular tachychardia (VT) to ventricular fibrillation (VF). We give an explanation for the experimental observation that there is a minimum tissue mass required for this transition to occur.

Key words **– Computer simulations, Reentry, VF and VT**

I. INTRODUCTION

Spiral waves of electrical activity in cardiac tissue are life threatening because they act as high frequency sources of waves that induce tachycardia, an abnormal rapid heart beat that is not controlled by the natural pace maker of the heart.

Once initiated in the ventricle, ventricular tachycardia (VT) usually decays within a few seconds into ventricular fibrillation (VF), a more spatiotemporally disorganized electrical activity leading to sudden cardiac death. Experiments in the heart using simultaneous multi-site electrode mappings as well as voltage sensitive dyes, have shown that in many cases VF is a consequence of several wandering spiral waves [1,2]. Therefore, it has been suggested that the rapid transition from VT to VF can be associated with the breakup of a spiral wave into multiple offspring [3,4] (see Fig. 1).

To understand this transition, there have been multiple and extensive studies of two-dimensional spiral waves and three-dimensional scroll waves in "isotropic" excitable media using various models, ranging from simple generic, to detailed ionic models with explicit membrane processes which accurately reproduce the cardiac action potential at the single cell level. [5]

Consequently a fair amount is known about their behavior, and several mechanisms for breakup have been found [3,4].

Nevertheless, very little is known about their behavior in bulk ventricular muscle (formed by cardiac fibers in which wave propagation is faster parallel to their axis than perpendicular to them and the fiber axis rotates transmurally across the ventricular walls).

Furthermore, none of the previously found breakup mechanisms occurring in isotropic excitable media can explain the results obtained in 1914 by Garrey [6], and multiple experiments thereafter, corroborating that a minimum mass of cardiac tissue seems to be necessary for the development of VT into VF.

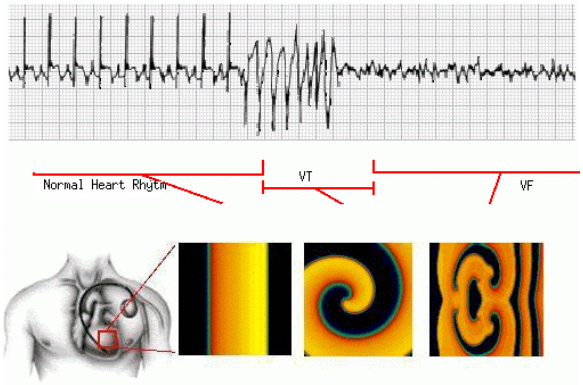

Fig. 1 Schematic representation of the transition from normal heart beat to ventricular tachycardia (VT) and then to ventricular fibrillation (VF) on an ECG recording.

The initiation of spiral waves (or reentrant waves) is relatively well understood. They can occur when the propagating electrical waves produce by the sino-atrial node are blocked by pre-existing fixed obstacles in the tissue [7] which have very little or no conduction at all such as scars, calcified plaques, or orifices.

Blocking of the wave can also be induce by residual obstacles of necrosis or poorly excitable myocardial regions produced by prior myocardial infractions.

In any case, the waves can then break and pin to this obstacles, propagating around them, in a topologically analogous way to plane wave propagation, with a period determined by the size of the obstacle and the conduction velocity [7].

Functional reentry is an alternate mechanism for the initiation of spiral waves, which in contrast to anatomical reentry, can occur in healthy tissue. In healthy tissue, reentrant spiral waves can be created and maintained, without obstacles or local inhomogeneities by functional conduction blocks caused by: (i) a non-uniform dispersion of repolarization produced by abrupt changes in stimulation rates and, (ii) unidirectional blocks created by stimuli induced at the same or other site.

Fig. 2 shows the initiation of spiral waves by a premature stimulation.

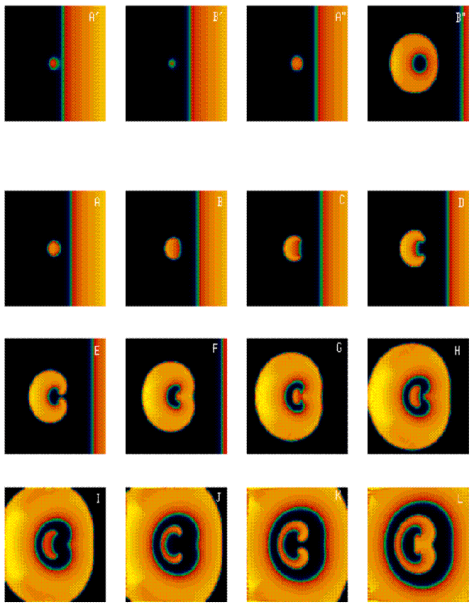

Fig. 2 Initiation of spiral waves by a premature stimulus. Dark areas represent unexcited tissue while yellow-red represents different levels of voltage excitation. Case 1 (panels A'-B'): shows a point premature stimulus that occurs too soon following a plane wave. The tissue behind the plane wave is refractory and the stimulus dies out. Case 2 (panels A"-B"): The premature stimulus occurs too late. The tissue behind the plane wave is readily excitable and the stimulus produces a bulls eye pattern wave. Case 3 (panels A-L) the premature point stimulus occurs successfully during the window of vulnerability producing two mirror image spiral waves of AP that rotate indefinitely. (See [8])

When a spiral wave is formed, the point where the front and the back of the wave meet is called the spiral wave tip. In 3D the spiral wave becomes a scroll wave and the tip-point becomes a line or "vortex filament" as shown in the results section. One characteristic of spiral wave dynamics is the trajectory of the spiral wave tip. Depending on the dynamical tissue characteristics, spiral wave tips can follow different types of paths [9], ranging from circular to linear trajectories with very sharp turns. Between these alternatives there is a gamut of trajectories that follow winding series of loop-like bends which turn upon themselves, and are known as meandering trajectories (see Fig. 3).

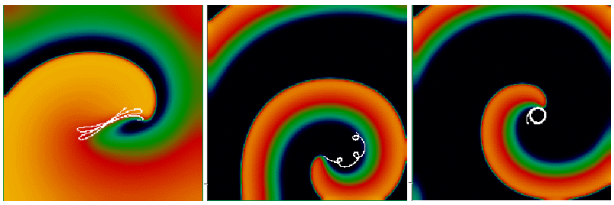

Fig 3 Color contour plots of action potential spiral waves in different regimes (from high to low excitability). Black regions represent polarized tissue and light regions depolarized. Linear, meander and circular trajectories have been noticed experimentally in cardiac tissue see for example [9].

II Restitution Curves

In cardiac tissue, it is possible to define two characteristic curves that describe how the duration and velocity of a wave depend on the time interval since the previous activation, during which the medium recovers its resting properties.

One is the APD restitution, which relates the duration the AP at a given point in the tissue, with the previous diastolic interval (DI) at the same point. This DI, or recovery time, measures the time between successive repolarization and depolarization of the cell membrane, measured at the same membrane potential threshold as the APD. The other is the conduction velocity (CV) restitution, which relates in similar way, the instantaneous conduction velocity of an excitation wavefront to the previous DI at the point where the velocity is measured. These two curves thus incorporate, in a functional form, the ionic complexity of the tissue as well as its electrophysiological characteristics.

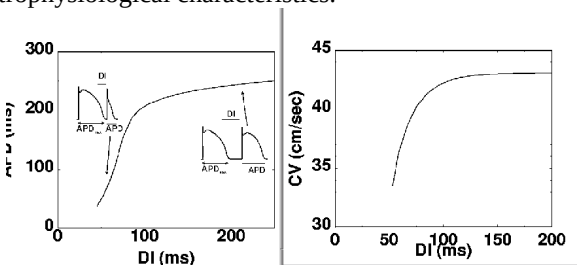

Fig. 4 A) APD restitution curve and B) CV restitution curve. In cardiac tissue there is a minimum DI for which there is no propagation of AP. It is the minimum time the cells need to recover before another excitation can be induced. These restitutions correspond to the BR model [5].

Numerical simulations with different models have shown that when the APD restitution curves is steep with slope > 1, breakup of spiral waves can occur by slow recovery fronts [3] and by APD oscillations [4]. Nevertheless, most experimental studies in normal tissue have reported APD restitution curves with slope < 1. Therefore it remains unclear whether steep restitution can occur only in diseased tissue, different protocols are needed to measure APD restitution, or whether other mechanisms are responsible for spiral wave breakup.

III The Ionic Model

To model the propagation of electrical activity and the dynamics of spiral waves in cardiac tissue. We use a simple ionic model [10], which is able to reproduce arbitrary monophasic generic and experimental APD and CV restitution curves. The total membrane current of the model is given by the sum of three independent phenomenological ionic currents: $I_t = I_{fi}(V;\boldsymbol{v}) + I_{so}(V) + I_{si}(V;\boldsymbol{w})$.

Where

(i) $I_{fi}(V;\boldsymbol{v})$ is a fast inward inactivation current used to depolarize the membrane when an excitation greater than threshold is induced. This current controls the CV restitution. It depends on the voltage V, an inactivation gate variable $\boldsymbol{v}$ and an activation gate that is extremely fast so it's replaced by a Heaviside step function. $I_{fi}(V;\boldsymbol{v}) = -\boldsymbol{v}(V-0.13)(1-V)p/\tau_d$. This current is directly analogous to the sodium current in more complex models such as the Beeler-Reuter (BR) and Luo-Rudy (LR) models [5].

(i) $I_{so}(V)$ is a slow time independent rectifying outward current used to repolarize the membrane back to the resting potential. This current is analogous to the time

independent potassium current in the BR and LR models [5]. $I_{so}(V)=V(1-p)/\tau_o + p/\tau_r$.

(iii) $I_{si}(V;\mathbf{w})$ is a slow inward inactivation current used to balance $I_{so}(V)$ and produce a plateau in the action potential. It depends on an inactivation gate variable of an activation gate variable. And can be consider analogous to the calcium current in the BR and LR models [5]. $I_{si}(V;\mathbf{w})=-\mathbf{w}(1+\tanh(10(V-0.85)))/2\tau_{si}$. These two currents control the APD restitution curve

In the model, the slow currents $I_{so}(V)$ and $I_{si}(V;\mathbf{w})$ are independent of the fast $I_{fi}(V;\mathbf{v})$ current. This gives the advantage of modeling the APD restitution curve independently from the CV curve. The gate variables follow a first order differential equation. $d_t\mathbf{v}(t)=(1-p)(1-\mathbf{v})/\tau_v^- - p\mathbf{v}/\tau_v^+$, $d_t\mathbf{w}(t)=(1-p)(1-\mathbf{w})/\tau_w^- - p\mathbf{w}/\tau_w^+$ and the membrane voltage propagates according to the cable equation $d_tV(t)=Dd_t^2V-I_t/C_m$. The 8 time constants τ_i and the Heaviside functions p and q are further described in [10].

While the dynamic characteristics of the tissue are included in the ionic current the static characteristics of the tissue are included in the diffusion term of the cable equation.

Dissection experiments in mammalian hearts [11] have shown that when the valves, the atrium and the thinner right ventricle, as well as the innermost fibers of the left ventricle, are removed, one ends up with a left ventricle that resembles a thick "cylinder". The myocardial fibers that form it are not exactly parallel to the epicardium, in fact they follow approximately geodesic paths that lie on nested families of toroidal surfaces within the heart wall [11]. This results on a fiber rotation with roughly constant rate, trough the cylinder walls [11].

In the model we included the effect of anisotropic fiber rotation using a thick slabs of cardiac tissue where the fibers rotate smoothly about 180^0 [11], and we include periodic boundary conditions when using a thin cylinder of cardiac tissue [12].

IV. Results

For all the simulations we started with a spiral wave formed in an equivalent way as a premature stimulus (See Fig. 2). The ionic parameters where chosen as to fit the ones of the Beeler-Reuter model with speedup Calcium (MBR) [3]. The spiral waves in this model (as well as with the original MBR) are stable in two dimensional tissues where the spiral tip follows a high meander trajectory [3].

PERIODIC BONDARY CONDITINS:

We found that as the spiral wave rotates on a thin cylinder with a large perimeter (compared with the meander trajectory) the dynamics is identical to the one of a spiral wave in a 2D plane tissue. However as the diameter of the cylinder is decreased and the perimeter becomes comparable to the spiral wavelength, then the spiral tip becomes perturbed by incoming waves generated by itself. When the cylinder diameter is comparable to the spiral wavelength, a drift on the spiral wave tip is induced by the collision of incoming waves with a higher frequency than the one of rotation [13]. This drift is independent of the tip trajectory as we checked by varying the spiral wave dynamics into the circular, and linear trajectory regimes shown in Fig. 3. As the cylindrical perimeter decreases, the spiral wave receives incoming waves at higher frequencies and the drift velocity increases. When the cylinder perimeter is further decreased and becomes smaller than the tip trajectory, there is no possibility for a sustained spiral wave. However for spiral waves in the hypermeander linear regime, there is an interesting window of cylindrical perimeter for which the drifting spiral will break up. Figure 5 shows a sequence of contour voltage plots of a spiral wave breakup on a small cylinder with perimeter 4.0 cm using the model fitted to the MBR.

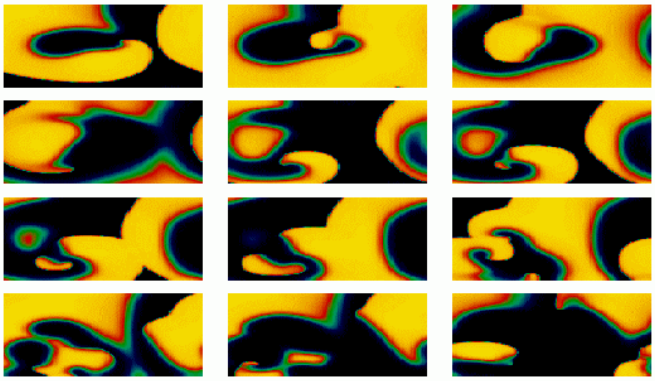

Fig. 5 Breakup of spiral waves due to periodic boundary conditions. Series of color contours of a spiral wave using the model fitted to MBR model on a cylinder with diameter of 4.0 cm. Sequence is from left to right and top to bottom. The vertical boundaries are the periodic ones, while the horizontal ones are zero flux. Notice the breakup due to conduction block between frames 5 and 6.

The breakup is produced because the hypermeander wave tip repolarizes unevenly some regions along the cylinder. Therefore, the incoming waves produced by itself can block the tip trajectory and form new spiral waves. Activations can disappear when the spirals are annihilated with the horizontal boundaries (zero current flux), however the conduction block is a repeatable cycle that keeps producing new waves.

The breakup of spiral waves due to periodic boundary conditions only depends on the tip meandering and the perimeter of the cylinder since we obtained similar breakup when using other models such as the real MBR model as well as the FHN model when in the linear core regime [12].

ROTATIONAL ANISOTROPY:

When a spiral wave was induced on a thick slab of tissue with rotational anisotropy we found that for thick tissues with little rotational anisotropy the vortex is stable to perturbations and behaves similarly as in a 2D plane sheet. However as the rotational anisotropy is increased for a fixed thickness, the vortex elongates and curves because of the twist induced by the rotational anisotropy. Fig. 6 Illustrate the nature of the twist that produces the filament instability. In the figure, twist is represented by plotting the normal vector to the spiral tip at equally spaced points along the filament. It can be seen that the normal vector changes orientation rapidly only along a short, and hence highly twisted, segment of the filament. The rise in twist amplitude takes place during the rapid pivot turn of the

spiral wave tip when tracing a meandering trajectory. This rise occurs because fiber rotation causes this pivot turn to take place asynchronously in different fiber sheets. This also produces that the localized twist travels through the vortex as shown in the figure. The intramural elongation and curving of the filament due to the twist, makes it collide with the boundaries of the muscle (*i.e.* the epicardium or endocardium). The original filament is cut into two segments. One that remains transmural and the other corresponding to a half vortex ring attached to the colliding surface. Subsequently, either the vortex rings contracts or it expands if sufficiently twisted. Fig 7 shows the second case where half rings expand, touch the other surface and further collisions leads to numerous vortices.

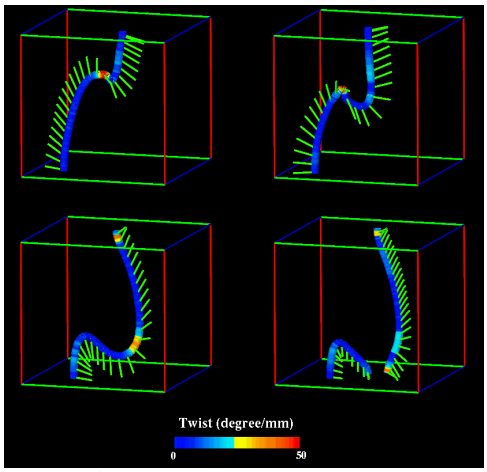

Fig 6 Propagation of twist along a spiral vortex line. Three-dimensional snapshots of a transmural vortex filament at different times. Note the localized twist traveling down until the vortex collides with the base froming a half ring. The speed of propagation is about 20 cm/s , the simulated tissue thickness is about 7.5 mm with a constant fiber rotation of 12^{o}/mm [10].

In this mechanism the number of vortices generated in the final state as well as the minimum wall thickness and fiber rotation threshold depend on the APD restitution curve. The stepper the curve the smaller is the minimum APD resulting in a bigger number of vortices in a given slab of cardiac tissue and conversely the flatter the APD restitution the harder is to induce the breakup.

V Conclusions

The spiral wave breakup due to periodic boundary conditions may be present in normal hearts when a hypermeander spiral wave is generated and/or it is drifted close to the apex where the perimeter of the heart is small. Also, the anisotropic fiber architecture of the left ventricular wall is a major predisposing factor for the degeneration of VT into VF. Our numerical simulations have demonstrated that transmural fiber rotation causes three-dimensional scroll waves to become unstable and to spontaneously decay into wave turbulence above a minimum wall thickness comparable to the one necessary to sustain ventricular fibrillation. The instability is characterized by the propagation of localized highly twisted and distorted regions of filaments along the electrical vortex filament and has no previously known analog in isotropic excitable media. When a vortex with a high twist collides with one of the natural boundaries of the ventricle it can create vortex rings. Moreover, when sufficiently twisted, these rings expand and create additional filaments by further colliding with boundaries, thereby leading to a turbulent wave state characteristic of fibrillation.

Movies for these breakup mechanisms can be found at:
`http://stardec.hpcc.neu.edu/~fenton/main.html`

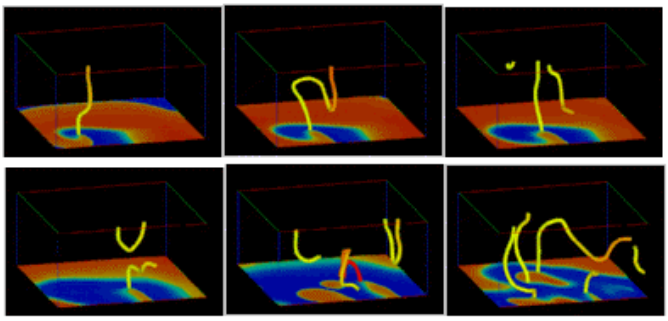

Fig 7 Three-dimensional snapshots showing the main creation events of vortex lines that lead to the decay of VT into VF. The bottom surface shows the voltage activation at that layer. As the vortex elongates (see Fig. 6) it touches the boundaries forming extra half rings which expand and produce new vortices and a complex spatio-temporal activity. (Same parameters as in Fig .6)

[1] P.S. Chen *et al.*, Chaos **8,** 127 (1998).
[2] M.J. Janse, Chaos **8**, 149 (1998).
[3] M. Courtemanche and A. Winfree, Int. J. Bifurcation Chaos. **1**, 431 (1991); M. Courtemanche, Chaos **6**, 579 (1996).
[4] A. Karma. Phys. Rev. Lett. **71**, 1103 (1993).
[5] G.W. Beeler and H. Reuter. J. Physiol. **268**, 177 (1977); C. Luo and Y. Rudy. Circ. Res. **68,** 1501 (1991).
[6] W.E. Garrey, Am. J. Physiol. **33,** 397 (1914).
[7] R.A. Gray and J. Jalife, Int. J. Bif. and Chaos **6,** 415 (1996).
[8] A.T. Winfree, When Time Breaks Down, Princeton Univ. Press, New Jersey, (1987).
[9] D.T. Kim et al., Chaos **8**, 137 (1998).
[10] F. Fenton and A. Karma, Chaos **8**, 20 (1998); Phys. Rev. Lett. **81**, 481 (1998).
[11] D.D. Streeter Jr. et al. Circ. Res. **24**, 339 (1969).
[12] F. Fenton, H. Hastings and S. Evans (to be publish).
[13] Y.A. Yermakova et al, Biophysics **31**, 348 (1986).

[1] Department of Mathematics, 103 Hofstra University, Hempstead, NY 11549-1030.
Fenton@rene.physics.neu.edu

[2] Department of Physics and Department of Mathematics, Hofstra University, Hempstead, NY 11549-1510.
Harold.Hastings@hofstra.edu

[3] Department of Physics, Northeastern University, Boston, MA 02115
Karma@presto.physics.neu.edu

[4] Beth Israel Medical Center, NY, NY
matsje@earthlink.net